Algorithm theoretical basis document (ATBD) for Normalized Fluorescence Line Height (nFLH) retrieval using EOS-6 (OCEANSAT-III) OCM

August 2025

S. No.	Product Name	Spatial Resolution (m)	Temporal Resolution
1	E06OCML2FL_YYYYMMDD_X_Y_Z_360m_LAC_v1.0.0.nc	360 m (LAC), 1km (GAC)	Alternate day

By

Debojyoti Ganguly and K. N. Babu
Biological Oceanographic Division
Atmospheric and Oceanic Sciences Group
Space Applications Centre, ISRO
Ahmedabad 380015, India

1	Date	September 2025
2	Title	Algorithm theoretical basis document (ATBD) for Normalized Fluorescence Line Height (nFLH) retrieval using EOS-6 (OCEANSAT-III) OCM
3	Type of Report	Technical - Algorithm Theoretical Basis Document (ATBD)
4	No. of Pages	
5	Authors	Debojyoti Ganguly and K.N. Babu
6	Originating Centre	Space Applications Centre (SAC)
7	Abstract	This document describes the algorithm for the generation of Normalized Fluorescence Line Height(nFLH) product from OCM-3. It uses the Level-2 operational Remote Sensing Reflectance (Rrs) and retrieves nFLH using the Fluorescence triplet channels by fiiting a straight line to the Fluorescence baseline bands and computing the residual signal above the baseline.
8	Keywords	OCM-3, nFLH, Rrs, nLw
9	Approving Authority	EPSA ATBD Review Committee
10	Classification	Unrestricted
11	Circulation	Open

Introduction:

Chlorophyll fluorescence is an important energy-release process after phytoplankton absorbs sunlight. When chlorophyll molecules absorb light fraction of the energy is released as light (fluorescence) in the far-red and near-infrared wavelengths (Erickson et al. 2019). This fraction depends on the incoming light intensity, photosynthetic efficiency, phytoplankton physiology, phytoplankton abundance and a host of other factors. Measuring the fluorescence signal provides an independent measurement of the amount of photosynthesis and phytoplankton biomass in the ocean. In oceanic case-1 waters, the water reflectance spectra is modulated by phytoplankton and its associated constituents, and thus the blue-green ratio algorithms for chlorophyll retrieval are observed to work well (Xing et al. 2007; Zhao et al. 2010). However, in case-2 coastal waters the optical properties of water are modulated not only by phytoplankton but also by the Colored Dissolved Organic Matter (CDOM), detritus, and suspended sediments. In such waters, the traditional blue-green ratio-based

chlorophyll algorithms become less efficient (Zhao et al. 2010). In such cases, fluorescence-based algorithms can be more useful (Neville and Gower, 1977; Gower et al. 1999). The fluorescence signal is primarily attributed to the presence of chlorophyll, as chlorophyll-a is the only pigment that causes emission in the far red and near-infrared wavelengths (Xing et al. 2007; Behrenfeld et al. 2009). Fluorescence line height (FLH) is a commonly used parameter to characterize the strength of the fluorescence signal.

FLH relies on three spectral bands for its estimation. The central wavelength corresponds to the maximum fluorescence signal (near 680 nm) and two baseline bands on each side of the fluorescence peak are used for estimating the FLH baseline. Nowadays, most modern ocean colour sensors have fluorescent bands (e.g., Moderate Resolution Imaging Spectroradiometer (MODIS) and the Ocean and Land Color Instrument (OLCI) aboard the polar-orbiting satellites, Aqua and Sentinel-3A/3B, respectively). Currently, MODIS is the only satellite sensor that gives operational FLH products using three FLH calculation bands which are 667, 678, and 748 nm. MODIS measures the upwelling radiance at 676.7 nm (bandwidth 673 to 683 nm, henceforth referred to as 678 nm waveband), whereas the fluorescence emission maximum is around 683 to 685 nm (Abbot and Letelier 1999 ; Huot et al 2005). This places the MODIS fluorescence peak wavelength closer to the absorption peak of chlorophyll-a at 676 nm (Huot et al. 2005).

The advantage of FLH as compared to standard chlorophyll products is mainly in case-2 coastal waters as well as high bloom conditions. In case-2 waters the dark pixel approximation for aerosol correction often fails as there is contribution from sediments and other optical constituents that backscatter in red and near infrared wavelengths. When the dark pixel approximation is used for atmospheric correction it overcorrects the spectra particularly the lower wavelengths mainly blue wavelengths. This may result in unusually low remote sensing reflectance in blue region and consequently high values of chlorophyll concentration. This problem is mitigated in FLH. Since FLH uses the chlorophyll fluorescence emission signal the errors due to atmospheric correction are much lesser.

1.1 OCEANSAT-III OCM Instrument

Ocean Colour Monitor (OCM)-3 on board EOS -06 is designed to measure spectral variation of water leaving radiances that can be related to bio-physical parameters like phytoplankton pigment concentration, diffuse attenuation coefficient (k_d), total suspended matter and coloured dissolved organic matter in ocean waters. The objective of EOS-6 Ocean Colour Monitor (OCM) is to continue the legacy of Oceansat-1 & 2 OCM by providing the quantitative information on bio-optical constituents such as chlorophyll-a concentration, vertical diffuse attenuation coefficient of light (K_d) at 490nm, total suspended matter etc., to the user community. OCM-3 has 13 bands in VNIR (400-1010 nm range) with 1440 km swath for ocean colour monitoring. OCM-3 will be operated in two modes such as a) Local Area Coverage (LAC) mode, to cater mainly for user's real-time requirement of high resolution data (360 m). b) Global Area Coverage (GAC) mode, to cover the global ocean at regular cycles in low

resolution mode (1 km). The spectral bands and technical specifications of OCM-3 and the corresponding values of OCM-1 and OCM-2 are specified in Table 1.

Table 1: Technical specifications of Ocean Colour Monitor onboard OceanSat-3

Band No.	**OCM-1 (centre wavelength)**	**OCM-2 (centre wavelength)**	**OCM-3 (centre wavelength)**
1	412 nm	412 nm	412 nm
2	443 nm	443 nm	443 nm
3	490 nm	490 nm	490 nm
4	510 nm	510 nm	510 nm
5	555 nm	555 nm	555 nm
6	640 nm	620 nm	566 nm
7	*765 nm	*740 nm	620 nm
8	*865 nm	*865 nm	670 nm
9			681 nm
10			710 nm
11			*780 nm
12			*870 nm
13			*1010 nm
No. of bands	8 bands	8 bands	13 bands
SNR (in visible bands)	~300	~300	800-1000

Overview and Background:

In order to carry out photosynthesis, phytoplankton contain several pigments. While the make up of these pigments differ depending on the species and other conditions, they all contain chlorophyll-a which is the primary pigment for photosynthesis. The chlorophyll molecule is strongly fluorescent with in-vivo fluorescence centred around 683 nm. When chlorophyll-a absorbs lower wavelength light it re-emits a fraction of the absorbed light as fluorescence. This fraction which is few percent of the absorbed light is the fluorescence quantum yield and depends on the phytoplankton species, intensity of incident radiation and also the phytoplankton physiology.

Chlorophyll fluorescence manifests as an added signal in the remotely sensed reflected spectra near the red wavelength (~683 nm). Quantification of this extra signal gives an estimate of the emitted signal due to chlorophyll fluorescence. As this signal is uniquely attributed to chlorophyll-a emission it can be used as a proxy for estimating phytoplankton abundance.

Algorithm description:

The input for nFLH is the Level-2 Remote Sensing Reflectance (Rrs) data of OCM-3. The Rrs data of OCM-3 is available in netCDF4 format for both Local Area Coverage (360 m) and Global Area Coverage (1km). Normalized Fluorescence Line Height (nFLH) is retrieved from Normalized Water

Leaving Radiance. Normalized water leaving radiance is the radiance that would exit the ocean in the absence of the atmosphere and with the sun at the zenith. Remote sensing reflectance at wavelength (λ) is expressed as

$$Rrs\ (\lambda) = \frac{L_w(\lambda)}{E_d(\lambda)} \quad (1)$$

Where L_w is the water leaving radiance and E_d is the downwelling irradiance just above the surface.

Level-2 Rrs is obtained after atmospherically correcting the Level-1C Top of the Atmosphere radiance by subtracting the effects of path radiance due to Rayleigh scattering and aerosol scattering. The sensor detected radiance can be expressed as (Kay et al. 2009).

$$L_{TOA} = L_{rayleigh} + L_{aerosol} + L_{ra} + TL_{glint} + tL_{whitecap} + tL_w \quad (2)$$

where $L_{rayleigh}$ is the path radiance due to the atmospheric gases, $L_{aerosol}$ is the scattering contribution due to the atmospheric aerosols, T is the direct transmittance, L_{glint} is the sun glint radiance , $L_{whitecap}$ is the whitecap contribution to radiance, t is the diffuse transmittance and L_w is the water leaving radiance.

In operational ocean colour products, sun glint is masked and the whitecap radiance is neglected as it is very minimal as compared to other terms (Ganguly et al. 2025). The aerosol and Rayleigh radiances are collectively known as the path radiance and can be estimated from the methodology given by Gordon and Wang (1994) and Gordon et al. (1988). The details about estimation of Rayleigh and aerosol radiance are provided in OCM-3 operational products Algorithm Theoretical Basis Document (Gupta et al. 2023). Once the terms associated with path radiance are estimated equation 2 can then be used for deriving water leaving radiance (L_w).

The normalized water-leaving radiance L_{WN} was defined by Gordon and Clark (1981) through

$$L_w(\lambda) = L_{WN}(\lambda) * \cos(\theta_0) * \exp\left[-\left(\frac{\tau_r(\lambda)}{2} + \tau_{oz}(\lambda)\right) * \left(\frac{1}{\cos(\theta_0)}\right)\right] \quad (2)$$

Where θ_0 is the solar zenith angle, τ_r (λ) and τ_{oz} (λ) are the Rayleigh and ozone optical thickness at wavelength λ.

Now the downwelling irradiance just above the ocean surface can be written as

$$E_d(\lambda) = F_0(\lambda) * \cos(\theta_0) * t \quad (3)$$

Where F_0 (λ) is the extraterrestrial solar irradiance at λ and t is the diffuse transmittance of the atmosphere given by

$$t = \exp[-\left(\frac{\tau_r(\lambda)}{2} + \tau_{oz}(\lambda)\right) * \left(\frac{1}{\cos(\theta_0)}\right] \quad (4)$$

From the above equations it can be seen that

$$L_{WN}(\lambda) = Rrs(\lambda) * F_0(\lambda) \quad (5)$$

For nFLH the OCM-3 bands centred at 670 nm, 680 nm and 710 nm are used. In open ocean the Rrs in these bands are very low. Sometimes negative values might also come due to errors in atmospheric correction, sensor radiometric sensitivity, sensor noise and other reasons. If negative Rrs or fill values are observed in any pixel, they are flagged and further processing is not done.

Before proceeding for nFLH computation from L_{WN}, it has to be noted that the chlorophyll fluorescence signal is very weak particularly in low chlorophyll open ocean regions and thus the nFLH imagery can be very noisy. In order to reduce the noise and improve the product quality a median filter is applied on the normalized water leaving radiance image, particularly for the bands that go in nFLH estimation. A median filter of kernel size 5*5 is applied on L_{WN} before nFLH computation. The following equation is used for nFLH (Gupta et al. 2025).

$$nFLH = L_f - [L_R + \frac{\lambda_R - \lambda_F}{\lambda_R - \lambda_L} * (L_L - L_R)] \quad (6)$$

Where, nFLH is the Normalized Fluorescence Line Height (FLH), L_R and L_L are the normalized water leaving radiance at wavelength λ_R and λ_L, respectively, which are the fluorescence baseline bands

Figure 1 shows an illustration of how nFLH is calculated from L_{WN} spectra.

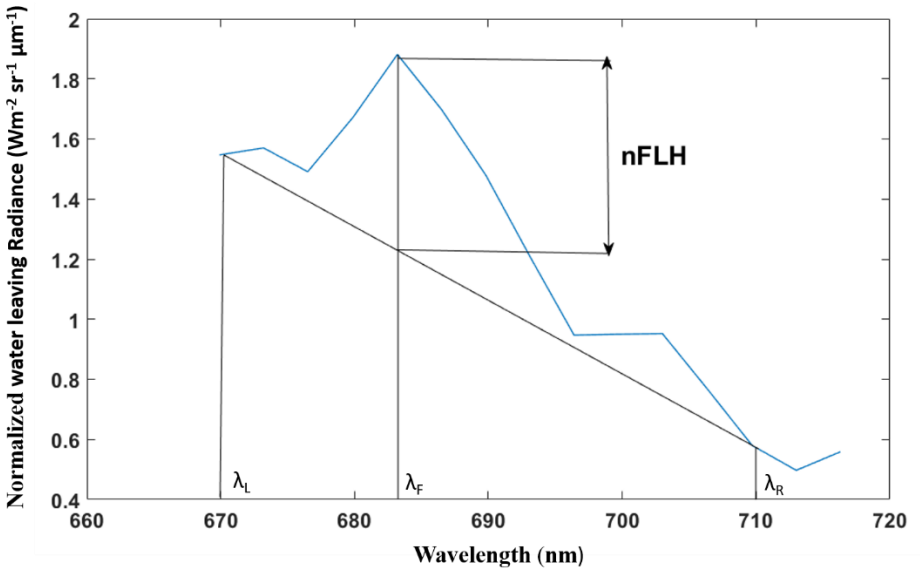

Figure 1: Fluorescence line height estimation using fluorescence baseline bands (λ_L and λ_R) and fluorescence peak emission band (λ_F). (Credits: Gupta et al. 2025).

As the fluorescence emission signal is very weak in open ocean, and the main application of nFLH is for case-2 coastal waters a mask based on ETOPO 1-minute bathymetry is used to mask out the open ocean areas. This is done as the noise in nFLH is very high particularly in low chlorophyll open ocean areas and the image port boundaries appear very prominent degrading the image quality in open ocean regions.

Results:

Figure 2 shows the chlorophyll as well as the nFLH image of coastal and offshore regions of Gujarat for 14 February 2023. It can be readily observed that the phytoplankton bloom like features are better captured in nFLH imagery as compared to chlorophyll imagery, particularly in coastal regions and also open ocean bloom regions. For the Gulf of Khambat region (black oval in Figure 2), the chlorophyll image shows absolutely no retrieval while valid retrieval is present in the nFLH imagery. This is because of failure of atmospheric correction in highly turbid and Colored Dissolved Organic Matter (CDOM) dominated waters. In turbid coastal waters the remotely sensed reflectance at Near Infrared (NIR) channels is non-zero and the dark pixel approximation fails. When the assumption of zero water reflectance is used it over-estimates the aerosol radiance. Consequently it over-corrects the spectra particularly at lower wavelengths. This can result in unusually elevated chlorophyll values in coastal areas. Figure 3 shows the chlorophyll and nFLH as obtained from OCM-3 for 13 February 2025. The limitation of standard chlorophyll product is clearly visible near coastal areas as chlorophyll image shows possible saturation and also lack of retrieval close to coast. The coastal features are better picked up in nFLH imagery for the same date.

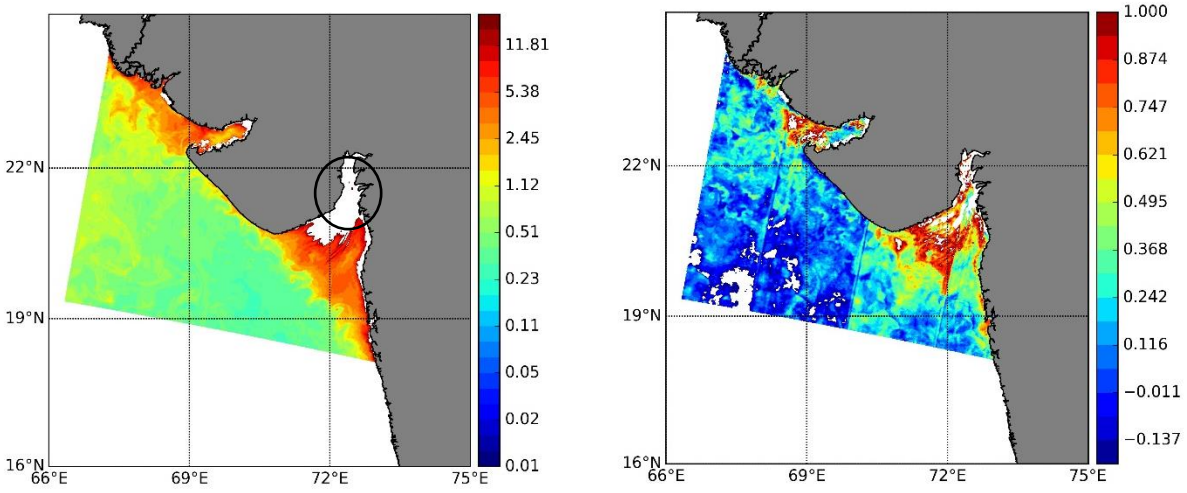

Figure 2: (a) OCM-3 chlorophyll concentration (mg/m^3) for 14 February 2023 (Path 57 Row 14), (b) OCM-3 nFLH (Wm^{-2}sr^{-1}µm^{-1}) for 14 February 2023 (Path 57 Row 14).

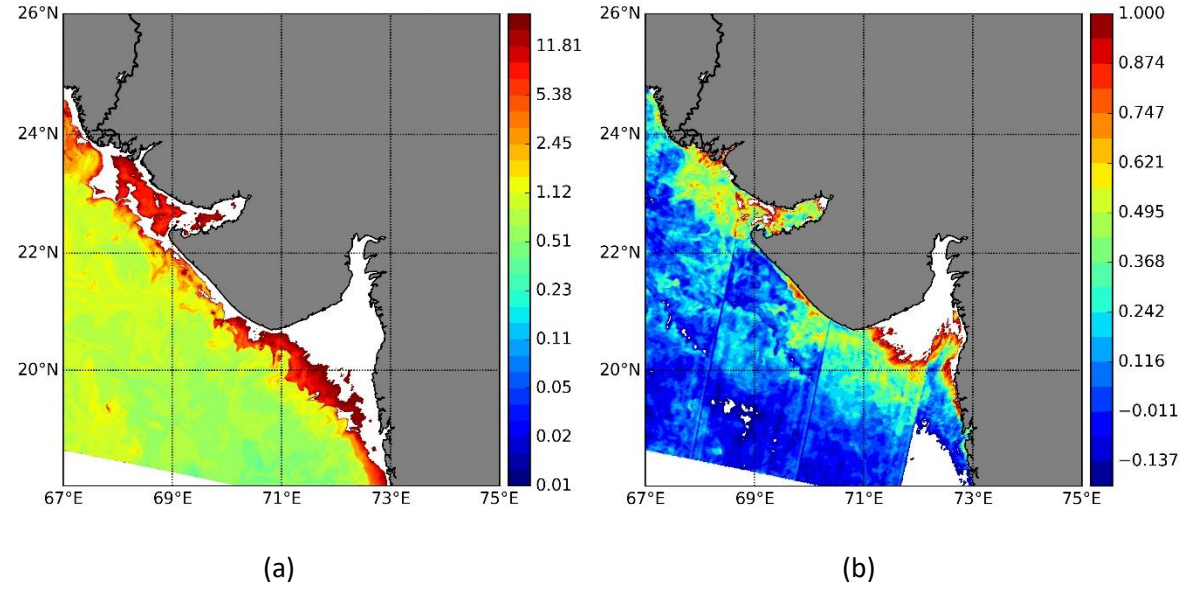

Figure 3: (a) OCM-3 chlorophyll concentration (mg/m^3) for 13 February 2025 , (b) OCM-3 nFLH (Wm^{-2}sr^{-1}µm^{-1}) for 13 February 2025.

Figure 4 shows the chlorophyll and nFLH for northern Bay of Bengal. Intense bloom like chorophyll concentrations with chlorophyll exceeding 10mg/m^3 are observed near Sunderban delta. Even here, the chlorophyll image shows data gaps due to failed retrieval particularly close to the coast. The nFLH image is able to better characterize the phytoplankton features in nearshore areas. The nearshore nFLH values reach more than 2 Wm^{-2}sr^{-1}µm^{-1}. The high nutrient influx from the Ganga, Brahmaputra and Meghna river systems results in high biological productivity in coastal and offshore areas. The high sediment loading from the river discharge can result in failure of the dark pixel approximation due to

non-zero water leaving reflectance in Near Infrared (NIR) channels. This can result in either over-estimation of chlorophyll or retrieval failure as discussed earlier.

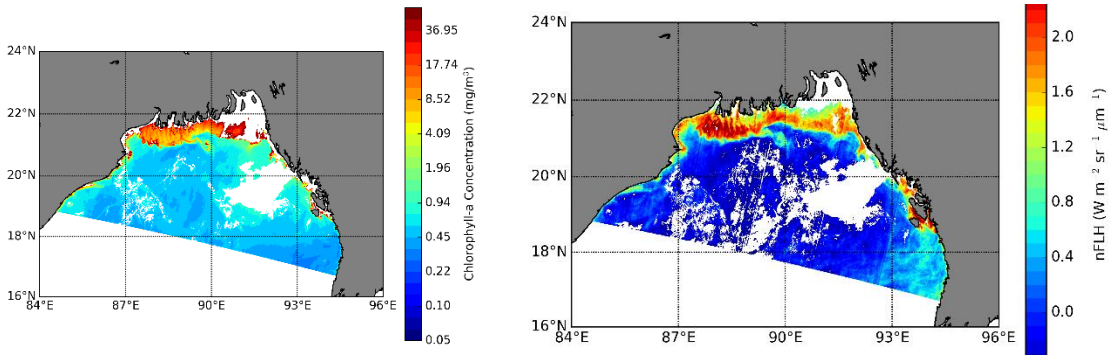

Fig. 4 (a) OCM-3 chlorophyll concentration (mg/m^3) for 21 February 2025 , (b) OCM-3 nFLH (Wm^{-2}sr^{-1}µm^{-1}) for 21 February 2025

Figure 5 shows the OCM-3 nFLH compared with Sentinel-3 OLCI nFLH for 8 February 2025 over Northern Bay of Bengal. The corresponding image histograms are also shown. It can be seen that nFLH from OCM-3 is very much in range as compared to OLCI derived nFLH in both open ocean as well as coastal. There is some difference between both histograms which could be because the image extent is somewhat different. Also, in open ocean the sun induced fluorescence emission is very weak and many a times below detection limits. Therefore, in low chlorophyll open ocean regions the nFLH is highly unreliable.

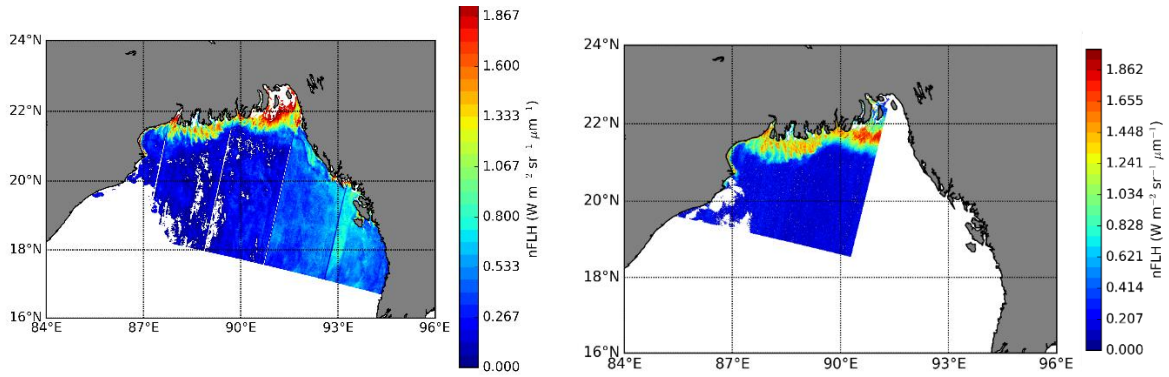

(a) (b)

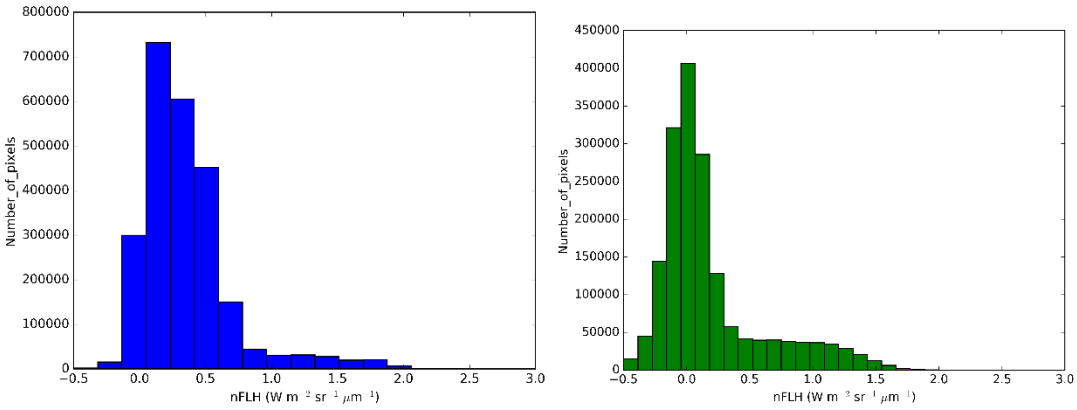

(c) (d)

Figure 5: (a) OCM-3 nFLH ($Wm^{-2}sr^{-1}\mu m^{-1}$) for 8 February 2025, (b) Sentinel-3 OLCI nFLH (($Wm^{-2}sr^{-1}\mu m^{-1}$) for 8 February 2025, (c) nFLH histogram of OCM-3 image, (d) nFLH histogram of OLCI image.

The northern Bay of Bengal particularly near Sundarban delta has high sediment loading from the riverine systems. This sediment loading can alter the optical properties of water particularly in the shallow coastal waters. The shallow coastal waters up to 50 m bathymetry are more prone to be affected by sediment dynamics. Thus, the nearshore chlorophyll product can be highly unreliable as it uses blue-green reflectance ratios which are likely to be affected due to the bright pixel nature of these turbid waters. The high sediment loading can also have an effect on the nFLH product and its retrieval accuracy. Thus, the nFLH product should be treated with caution in highly turbid coastal and estuarine waters due to high scattering in red and NIR wavelengths. Nevertheless, the nFLH product is more reliable as compared to blue-green chlorophyll in low to moderate turbid waters.

From the figures, it can be seen that there is significant banding in the open ocean areas which may degrade the visual quality of image and also affect the features and quantitative values near port boundaries. As the main application of nFLH is for case-2 coastal waters we intend to mask out nFLH beyond 500 metres bathymetry using ETOPO-1 bathymetry. Level-2 nFLH would be operationally generated in MOSDAC after the masking. Figure 6 shows the nFLH imagery for 1 January 2025 for Arabian Sea after applying the bathymetry mask. It can be observed that the high chlorophyll fluorescence areas can be easily distinguished from the offshore low fluorescence areas.

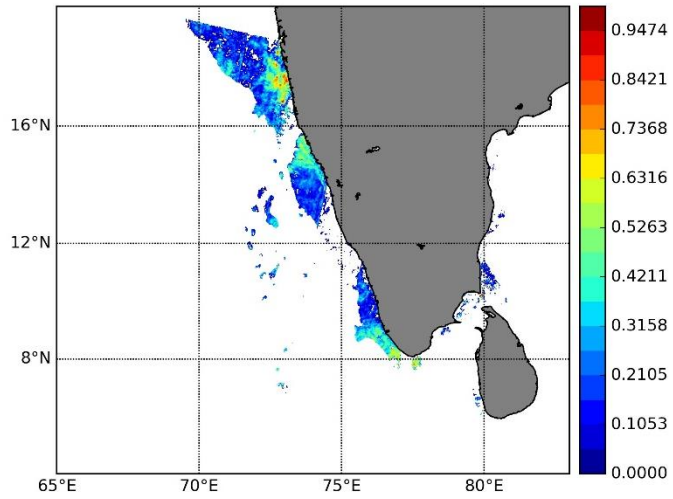

Figure 6: OCM-3 nFLH for 1 January 2025 after applying open ocean mask.

Validation of OCM-3 nFLH product:

nFLH obtained from OCM-3 can be validated either with other state of the art sensors or with nFLH derived from in-situ Rrs. Figure 7 shows the validation scatter along with validation statistics of OCM-3 nFLH with Sentinel-3 Ocean and Land Colour Imager (OLCI) nFLH in Mandovi estuary for collocated sampling points. The sampling points were collected on 14/1/2024 and 21/1/2024 in Zuari/Mandovi estuary. It can be observed that nFLH from OCM-3 is found to be reasonably correlated with OLCI nFLH with RMSE of 0.08 $Wm^{-2}sr^{-1}\mu m^{-1}$. The difference in nFLH could be attributed due to differences in spectral bandwidths, central wavelengths of fluorescence bands, difference in time of satellite overpass and several other sensor and processing related differences. Nevertheless, the nFLH product of OCM-3 is able to capture open ocean blooms and coastal blooms quite reasonably.

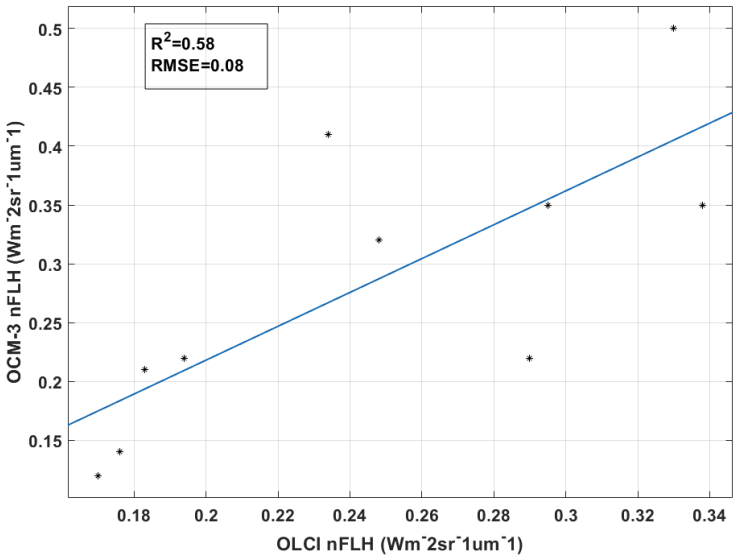

Figure 7: Validation scatter of OCM-3 nFLH with OLCI nFLH in Mandovi estuary

Limitation and Future Scope:

As the emitted fluorescence signal is very low the port boundaries appear very prominent and degrade the quality of the image particularly near port edges. In current version of ATBD nFLH would only be made available up to 500 m bathymetry from coast. This version of products would be hosted on Meteorological and Oceanographic Satellite Data Archival Centre (MOSDAC) data portal of Space Applications Centre (SAC) and the quality of products assessed. In future versions if the port imbalance problem is mitigated and the nFLH image appears less noisy, the product can be provided for the entire Level-2 scene.

Acknowledgments:

We express our sincere thanks to Director-Space Applications Centre Shri Nilesh Desai, Deputy Director-EPSA/SAC, Dr. Rashmi Sharma and Group Director-AOSG/EPSA Dr. Pradeep Kumar Thapliyal for their continuous support during this study

References:

1) Abbot, M.R., & Letelier, R.M. (1999). Algorithm theoretical basis document chlorophyll fluorescence (MODIS product number 20), NASA (http://www.modis.gsfc.gov/data/atbd).

2) Behrenfeld, M.J., Westberry, T.K., Boss, E.S., O'Malley, R.T., Siegel, D.A., Wiggert, J.D., Franz, B.A., McClain, C.R., Feldman, G.C., Doney, S.C., Moore, J.K., Dall'Olmo, G.,

Milligan, A.J., Lima, I., & Mahowald, N. (2009). Satellite-detected fluorescence reveals global physiology of ocean phytoplankton. *Biogeosciences*. 6(5): 779-794.

3) Erickson Z.K., Frankenberg, C., Thompson, D.R., Thompson, A.F., & Gierach, M. (2019). Remote Sensing of Chlorophyll Fluorescence in the Ocean using Imaging Spectrometry: Toward a Vertical Profile of Fluorescence. *Geophysical Research Letters*. 46(3): 1571-1579. https://doi.org/10.1029/2018GL081273.

4) Ganguly, D., Babu, K.N., & Gupta, A. (2025). Evaluation of the Sun-Glint Masking Algorithm on OCM-3 Operational Products and Impact of Using Simultaneous Sea Surface Winds Available from Scatterometer Onboard EOS-06 Satellite. *J. Indian Soc. Rem. Sens.* Pp:1-18.

5) Gower, J.F.R., Doerffer, R., & Borstad, G.A. (1999). Interpretation of the 685 nm peak in water leaving radiance in terms of fluorescence, absorption and scattering, and its observation by MERIS. *Int. J. Remote Sens*., 20, 1771-1786. https://doi.org/ 10.1080/014311699212470.

6) Gupta, A., Ganguly, D., Sahay, A., Prasad, T.D., Nagamani, P.V. & Raman, M. 2023 Algorithm theoretical basis document (ATBD) for Geophysical parameter retrieval using EOS-6 (OCM), EPSA/BPSG/MED/ATBD30.

7) Gupta, A., Ganguly, D., Babu, K.N., Raman, M., Thapliyal, P.K., & Sharma, R. (2025). Role of Additional Bands in Ocean Colour Monitor (OCM) on Board EOS-06 in Arabian Sea Near Gujarat Coast. *J. Indian Soc. Rem. Sens*. Doi: 10.1007/s12524-025-02218-8.

8) Huot, Y., Brown, C.A., & Cullen, J.I. (2005). New algorithms for MODIS sun-induced chlorophyll fluorescence and a comparison with present data products. *Limnol. Oceanogr: Methods*. 3, 108-130

9) Neville, R.A. & Gower, J.F.R. (1977). Passive remote sensing of phytoplankton via chlorophyll fluorescence. *J.Geophys. Res*., 82, 3487-3493. https://doi.org/ 10.1029/jc082i024p03487.

10) Xing, X.G., Zhao, D.Z., Liu, Y.G., Yang, J.H., Xiu, P., & Wang, L. (2007). An overview of remote sensing of chlorophyll fluorescence. *Ocean Science Journal*. 42: 49-59.

11) Zhao, D., Xing, X., Liu, Y., Yang, J., & Wang, L. (2010). The relation of chlorophyll-a concentration with the reflectance peak near 700 nm in algae-dominated waters and sensitivity of fluorescence algorithms for detecting algal bloom. Int. J. Rem..Sens. 31(1): 39-48.